Modeling the Growth and Formation of Instabilities During Spherical Flame Propagation

C. Regis Bauwens[a,b], Jeffrey M. Bergthorson[b], Sergey B. Dorofeev[a]
[a]FM Global, Research Division, Norwood, USA
[b]Department of Mechanical Engineering, McGill University, Montreal, Canada

1 Introduction

When evaluating the consequences of accidental explosions, accurate prediction and modeling of the rate of flame propagation is crucial for hazard assessment. In a freely expanding spherical configuration, however, the growth of the Darrieus-Landau instability [1, 2] results in significant flame acceleration. Characterization of this flame acceleration is needed to properly capture the behavior of large scale flames.

While many analytical studies have been performed to describe the growth of flame instabilities on a spherical flame [3, 4, 5], those studies have focused on the onset of instability and not the resulting flame acceleration. To describe the mechanism of spherical flame acceleration, the concept of self-similar flame propagation has been used by Gostintsev et al. [6] considering the increase in flame surface area due to the growth and splitting of cells as the flame radius increases. In previous studies [7, 8], oscillations in the rate of flame acceleration were observed, consistent with the underlying concept of self-similar flame propagation, suggesting the growth and formation of discrete length scales of instabilities during spherical flame propagation.

In this study, a simple model describing the growth of multiple generations of cells on a flame surface is developed and compared with experiments from a previous study. In future work, this approach may be used to quantify the parameters responsible for spherical flame acceleration.

2 Model Description

The general modeling approach considers the growth of each generation of cells on the flame surface independently, with a growth rate relation consistent with the results of linear stability

Correspondence to: carl.bauwens@fmglobal.com

analysis. The cells reach an equilibrium amplitude due to flame annihilation at cusps using a similar approach seen in the literature [9]. Cell splitting and the formation of additional length scales is modeled to occur when the local stretch rate drops below a critical stretch rate, k_c, and form cells with a critical wavelength of instability, Λ_c. These cells are assumed to be stationary on the surface and grow self-similar with the overall flame radius. The superposition of the multiple length scales of cells is used to obtain the flame surface wrinkling, Ξ, the ratio of surface area between a cellular flame and a smooth unwrinkled flame. And the propagation velocity of the flame is taken to be the laminar flame speed times this flame surface wrinkling factor.

2.1. Growth of a single generation of cells:

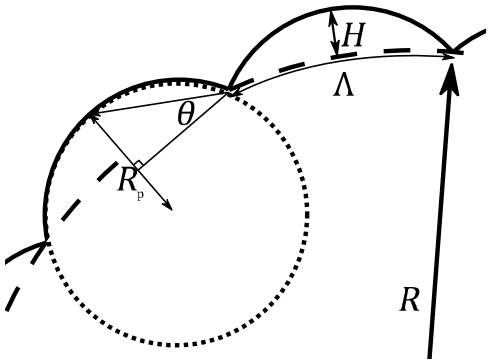

Figure 1. Schematic of the flame surface.

Figure 1 shows a schematic of the flame surface where H and Λ are the height and length of a cell, respectively, R and R_P are the radius of curvature of the overall flame and leading edge of the cell, respectively, and θ is the angle of a newly forming cell relative to the direction of flame propagation.

For the purpose of the model, a parabolic profile for the flame cross-section is assumed, given by:

$$y = a\Lambda\left(1 - \left(\frac{2x}{\Lambda}\right)^2\right), \tag{1}$$

where a is a dimensionless amplitude, $a = H/\Lambda$ and x is the position in the cell with a range $-\Lambda/2 < x < \Lambda/2$. The increase in flame surface area relative to a spherical profile can be estimated as the ratio of the surface area of a paraboloid to its base:

$$\Xi = \frac{1}{3a^2}\left[\left(\frac{1}{4} + 4a^2\right)^{3/2} - \frac{1}{8}\right]. \tag{2}$$

It is interesting to note that Eq. (2) is independent of the length scale of the cell and only varies with the dimensionless amplitude.

The dimensionless growth rate of the cell was modeled using an approach similar to that described in [9]:

$$\frac{dh}{d\tau} = G^* u_{\mathrm{F}}^* a - 8 u_{\mathrm{F}}^* a^2, \tag{3}$$

where h is the cell height normalized by the flame radius at the onset of instability R_{c}, τ is time normalized by the critical stretch rate, k_{c}, G^* is a coefficient of proportionality that is determined through comparison with previous experiment results [8], and u_{F}^* is the laminar flame speed of the mixture normalized by $R_{\mathrm{c}} k_{\mathrm{c}}$:

$$u_{\mathrm{F}}^* = \sigma S_{\mathrm{L}} / (R_{\mathrm{c}} k_{\mathrm{c}}) \left(1 - \frac{L_{\mathrm{M}}}{R_{\mathrm{F}}}\right), \tag{4}$$

where σ is the expansion ratio, S_{L} is the laminar burning velocity, L_{M} is the Markstein length and R_{F} is the flame radius. For the purpose of this model, $R_{\mathrm{F}} = R$ for the initial smooth flame and $R_{\mathrm{F}} = R_{\mathrm{P}}$ once the instability forms. It should be noted that while the Markstein length was used throughout the analysis, the results were largely insensitive to its value. In terms of the dimensionless amplitude, Eq. (3) can be expressed as:

$$\frac{da}{d\tau} = \frac{n u_{\mathrm{F}}^*}{2\pi r} (G^* a - 8a^2) - \frac{a}{r} \frac{dr}{d\tau} \tag{5}$$

where n is the number of cells around the flame radius given by $n = 2\pi r / \lambda_{\mathrm{c}}$, $r = R/R_{\mathrm{c}}$ and $\lambda_{\mathrm{c}} = \Lambda_{\mathrm{c}} / R_{\mathrm{c}}$.

2.2. Combining multiple wavelengths

To model cell splitting and the growth of subsequent generations of cells on the flame surface, additional assumptions must be made. As the primary stabilization mechanism that controls the onset of instability is the stretch rate [9], it is used as the criteria for cell splitting. In this model, the critical stretch rate for cell splitting is assumed to be constant across each generation of cells and this value is extracted directly from the onset of flame instability observed in experiments.

While the stretch rate for a smooth spherical surface can be described as: $k = \frac{1}{A} \frac{dA}{dt}$, where A is the surface area of the flame, the overall surface area of a cellular flame cannot be used to determine the local stretch rate at the leading edge of a cell. Instead, the local radius of curvature is used, which is given by the following, for a parabolic profile:

$$r_{\mathrm{p}} = \frac{\pi r}{4an}. \tag{6}$$

Calculating the stretch rate using the above relationship yields the following expression for the dimensionless stretch rate, $\kappa = k / k_{\mathrm{c}}$:

$$\kappa = \frac{2}{a} \frac{da}{d\tau} + \frac{2}{r} \frac{dr}{d\tau}. \tag{7}$$

2.4. Total flame surface area

To estimate the overall flame surface area generated by multiple length scales of wrinkles, a linear superposition of each wavelength is assumed, as shown in Fig. 2.

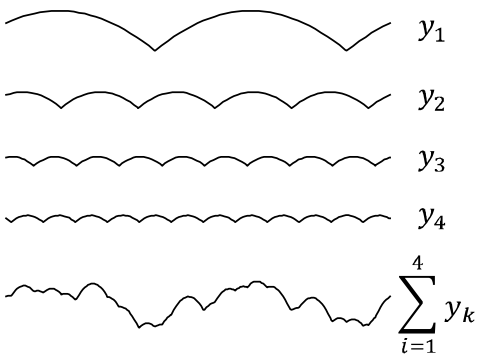

Figure 2. Combining multiple length scales of instability

The increase in flame surface wrinkling for a given set of wavelengths, however, varies heavily depending on the phase difference between modes, and no closed form analytical solution can be obtained for an arbitrary combination of parameters. Instead, a relationship for total flame surface area, Ξ_{T}, as a function of the individual length scales, Ξ_i, was obtained through numerical integration of the combined flame profile, averaged over a population of 10,000 stochastically varied combinations of the input parameters up to $i = 50$.

From this approach, it was found that the Ξ_{T} can be estimated from the contribution of each generation using the following relationship:

$$\Xi_T = \left[\sum(\Xi_i - 1)^{\beta}\right]^{1/\beta} + 1, \tag{8}$$

where the value β varies with the average amplitude of each node. For the typical range of a seen in this study, a value of $\beta = 1.4$ was found to agree with the results of the numerical integeration to within a standard deviation of the averaged results.

2.5. Effect of multiple generation of cells on cell growth

Additional effects are taken into account due to the presence of multiple generations of cells. First, a factor, Θ is introduced to account for the reduction in both the generation and removal rate terms in Eq (5) due to the angle of the cell relative to the overall propagation direction of the flame. This factor is approximated as:

$$\Theta = \prod_{k=1}^{k=i-1} \frac{1-4a_k^2}{2} \tag{9}$$

Another effect considered is the increase in cusp angle, and removal rate, due to cell splitting and the growth of a new generation. This is approximated as:

$$R_i^* = \frac{\Lambda_{i+1}}{\Lambda_{\mathrm{c}}}. \tag{10}$$

This factor produces the oscillations in the rate of flame acceleration in the model. These terms are incorporated in Eq. (5) as follows:

$$\frac{da_i}{d\tau} = \Theta \frac{n_i u_F}{2\pi r}(G^* a_i - 8R_i^* a_i^2) - \frac{a_i}{r}\frac{dr}{d\tau} \quad (11)$$

3 Results/Discussion

For direct comparison of the model with a previous methane-air study [8], a number of inputs are needed. The expansion ratio σ was obtained from chemical equilibrium, L_{M} was obtained from the literature [10] and values of S_{L} and k_{c} were extracted directly from experimental results.

The remaining parameters of G^* and Λ_{c}, however, cannot be determined directly from the experiments. An observation from the previous study, however, that u_{F}^* collapses to a single curve for mixtures with positive Markstein length [7] can be used to gain further insight into these parameters. This relationship imposes two significant restrictions, first, the equilibrium values of a must be constant across the mixtures, meaning the ratio of growth rate to removal rate terms in Eq. (11) must be constant. As the removal rate is only a function of a, this implies that G^* is constant across mixtures as well, which is consistent with theory as G^* varies weakly with the expansion ratio and laminar burning velocity of the flame [9]. Secondly, Eq. (11) shows that if G^* is constant, the frequency of the oscillations will only align if the value of n_{c} is constant across the mixtures, which can be used to define Λ_{c}.

It was found that values of $G^* = 3.1$ and $n_{\mathrm{c}} = 25$ produced results agreement across the full range of experimental results, as shown in Fig. 3. Reasonably good agreement was seen for all three mixtures in terms of the overall propagation velocity and frequency of oscillation. In addition, other features, such as the larger increase in velocity for the first generation of cells, the decrease in slope for each subsequent generation, and the cell splitting interval were also reproduced. The model does under-predict the experimental results at larger radii, however, which is likely due to effects such as radiation and the flame approaching the chamber walls.

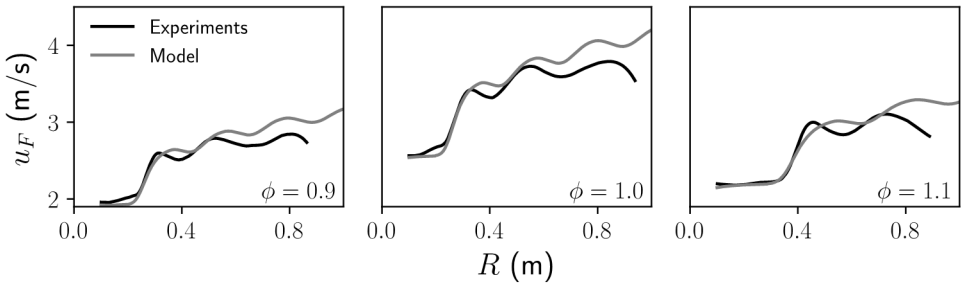

Figure 3. Comparison of model results with experiments for flame velocity as a function of radius.

Normalizing the flame velocity by the laminar flame speed, the model collapses to a single curve and can be compared over a wider range of experiments as shown in Fig. 4. This shows that the model captures the global behavior of the flame across the full range of experimental results.

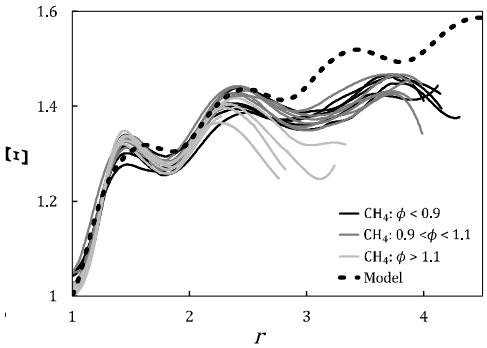

Figure 4. Comparison of model results across the full range of experiments [8].

4 Conclusions

A simple model was developed to describe spherical flame acceleration considering the growth of multiple length scales of wrinkles. The model captures a number of features observed in the experiments including oscillatory flame acceleration and the correct splitting interval. It is also found that the form of the model implies that the critical number of cells forming on the flame surface was constant across the range of mixtures examined with positive Markstein length. These results support the self-similar argument of spherical flame acceleration and can be used to develop new parameters to describe the behavior of large scale flames.

References

[1] Darrieus G. unpublished work presented at La Technique Moderne, and at Le Congrès de Mécanique Appliquée (1945) and (1938)

[2] Landau LD. (1944). On the theory of slow combustion. Acta Physicochim. URSS, 19(1): 77.

[3] Bradley D. (1999). Instabilities and flame speeds in large-scale premixed gaseous explosions. Phil. Trans. Royal Soc. A. 357(1764): 3567.

[4] Bechtold JK, Matalon M. (1987). Hydrodynamic and diffusion effects on the stability of spherically expanding flames. Combust. Flame. 67(1): 77.

[5] Sivashinsky GI. (1979). On self-turbulization of a laminar flame. Acta Astronaut. 6(5-6): 569.

[6] Gostintsev YA, Istratov AG, Shulenin YV. (1988). Self-similar propagation of a free turbulent flame in mixed gas mixtures. Combust., Explosion, and Shock Waves. 24(5): 563.

[7] Bauwens CR, Bergthorson JM, Dorofeev SB. (2015). Experimental study of spherical-flame acceleration mechanisms in large-scale propane–air flames. Proc. Combust. Inst. 35(2): 2059.

[8] Bauwens CR, Bergthorson JM, Dorofeev SB. (2016). On the interaction of the Darrieus–Landau instability with weak initial turbulence. Proc. Combust. Inst. 36(2): 2815

[9] Zel'dovich Ya B, Barenblatt, GI, Librovich, VB, Makhviladzw GM. (1985). The mathematical theory of combustion and explosions. Plenum Publishing Corporation (ISBN 0-306-10974-3).

[10] Taylor SC. (1991). Burning velocity and the influence of flame stretch (Doctoral dissertation, University of Leeds).